Journal of Advanced Ceramics
2014, 3(4): 278–286
DOI: 10.1007/s40145-014-0119-8

ISSN 2226-4108
CN 10-1154/TQ

Research Article

Abrupt change of dielectric properties in mullite due to titanium and strontium incorporation by sol–gel method

Biplab Kumar PAUL, Kumaresh HALDAR, Debasis ROY, Biswajoy BAGCHI, Alakananda BHATTACHARYA, Sukhen DAS*

Physics Department, *Jadavpur University*, *Kolkata-700 032*, *India*

Received: March 24, 2014; Revised: June 16, 2014; Accepted: July 06, 2014

Abstract: Highly crystallized mullite has been achieved at temperatures of 1100 ℃ and 1400 ℃ by sol–gel technique in presence of titanium and strontium ions of different concentrations: $G_0 = 0$ M, $G_1 = 0.002$ M, $G_2 = 0.01$ M, $G_3 = 0.02$ M, $G_4 = 0.1$ M, $G_5 = 0.2$ M and $G_6 = 0.5$ M. X-ray diffraction (XRD), Fourier transform infrared spectroscopy (FTIR), field emission scanning electron microscopy (FESEM), LCR meter characterized the samples. Mullite formation was found to depend on the concentration of the ions. The dielectric properties (dielectric constant, loss tangent and AC conductivity) of the composites have been measured, and their variation with increasing frequency and concentration of the doped metals was investigated. All the experiments were performed at room temperature. The composites showed maximum dielectric constants of 24.42 and 37.6 at 1400 ℃ of 0.01 M concentration for titanium and strontium ions at 2 MHz, respectively. Due to the perfect nature of the doped mullite, it can be used for the fabrication of high charge storing capacitors and also as ceramic capacitors in the pico range.

Keywords: mullite; sol–gel technique; X-ray diffraction (XRD); dielectric properties; field emission scanning electron microscopy (FESEM)

1 Introduction

Mullite is a promising engineering ceramic material for use in optical, dielectric and structural applications. Mullite has a unique combination of properties, such as high melting point (1830 ℃), good electrical resistance, good mechanical strength, low thermal expansion coefficient, high strength and high creep resistance at any temperature range. Mullite is also a leading candidate material for high transmitting IR windows, electronic substrates, humidity sensors, protective coatings, electrical insulators and turbine engine components, etc.

Electronic industry is continuously trying to develop processes that are more advanced and lead to forecasting transistor density and chip complexity, and operating speed or frequency for future technological developments [1,2]. The main challenge is to carry electric power and distribute clock signals that control the timing and synchronize the operation. This challenge extends beyond the material properties and technology and also involves system architecture [3–7]. Controlled chip connections used in high package density logic devices require a good compatibility of thermal expansion coefficient (TEC) between substrate and Si chip. The mullite composite system has required

* Corresponding author.
E-mail: sdasphysics@gmail.com

strength and much closer match of TEC with Si chip than alumina.

Several reports have been published dealing with synthesis of mullite composites in presence of various mineralizing agents to improve the mechanical and chemical properties, and also there are some recent publications related to the dielectric properties of these modified mullite composites [8–14]. We have studied the dielectric constant, loss tangent, AC conductivity of the mullite composites doped with varying concentrations of tungsten ions with different frequencies at room temperature. We also have studied the dielectric constant, loss tangent, AC conductivity and magnetization of the mullite composites doped with varying concentrations of iron ions with different frequencies at room temperature. The results indicate that the sample of 0.01 M concentration has the highest dielectric constant 24.42 at frequency 2 MHz [15,16].

2 Experimental

2.1 Sample materials

Chemicals used in the preparation of mullite precursor gels were aluminium nitrate nonahydrate ($Al(NO_3)_3{\cdot}9H_2O$, MERCK, India, 99.9%), aluminium isopropoxide ($Al(–O–i–Pr)_3$, puriss, Spectrochem Pvt. Ltd., India), tetraethyl orthosilicate ($Si(OC_2H_5)_4$, TEOS, MERCK, Germany), titanium isopropoxide ($Ti\{OCH(CH_3)_2\}_4$, MERCK, Germany, 99.9%) and strontium chloride hexahydrate ($SrCl_2{\cdot}6H_2O$, MERCK, India, 99.9%).

2.2 Sample preparation and characterization

Mullite precursor gel powder was synthesized by dissolving stoichiometric amounts of $Al(–O–i–Pr)_3$ and TEOS in 0.5 M solution of $Al(NO_3)_3{\cdot}9H_2O$ [12,13]. The molar ratio of $Al(–O–i–Pr)_3$: $Al(NO_3)_3{\cdot}9H_2O$ was kept at 3.5∶1. The molar ratio of Al∶Si was 3∶1 [12,13].

For preparation of the doped gels, the titanium and strontium salts were added to the original solution in the ratio of Al∶Si∶x, where x is the concentration of the metal salts in molarity. The titanium and strontium salts were added such that in the final solution x = 0.002 M (G_1), 0.01 M (G_2), 0.02 M (G_3), 0.1 M (G_4), 0.2 M (G_5), 0.5 M (G_6) [12,13]. The sol would be in the gel form after vigorous stirring for 5 h, and the sol was maintained overnight at 70 ℃. Finally, the gel was dried at 120 ℃. The samples were then pelletized and sintered at 1100 ℃ and 1400 ℃ or 3 h in a muffle furnace under air atmosphere (heating rate 10 ℃/min) [12,13].

2.3 Instruments used

The crystalline phases developed in the samples sintered at 1100 ℃ and 1400 ℃ were analyzed by X-ray powder diffractometer (XRD, model-D8, Bruker AXS, Wisconsin, USA) using Cu Kα radiation at 1.5418 Å and operating at 40 kV with a scan speed of 1 s/step.

The characteristic stretching and bending modes of vibration of chemical bonds of a sample can be effectively evaluated by spectroscopic methods. 1% of the sample was mixed with spectroscopy grade KBr, pelletized to form disc and analyzed by Fourier transform infrared (FTIR) spectroscopy (FTIR-8400S, Shimadzu).

AC parameters such as capacitance (C) and dissipation factor ($\tan\delta$) of the samples were measured in the frequency range of 20 Hz to 2 MHz using LCR meter (HP Model 4274 A, Hewlett-Packard, USA). The variation of dielectric constant and loss tangent was studied by recording these parameters using sample pellets of uniform thickness at ten different frequencies from 20 Hz to 2 MHz.

Morphology of the sintered gels was observed by field emission scanning electron microscopy (FESEM, JSM 6700F, JEOL Ltd., Tokyo, Japan). Samples were etched with 25% HF solution. About 2 mg of each sample was dispersed in ethanol, and a single drop was placed on copper grid for sample preparation.

3 Results and discussion

From the X-ray diffractograms, it can be seen that the undoped sample shows considerable mullite phase at 1100 ℃ and 1400 ℃, while for the doped samples, prominent mullite peaks are also obtained and changing with the concentrations. Mullite phase (JCPDS No. 150776) increases with increasing concentration of metal ions (Figs. 1 and 2). From the diffractograms, it has been observed that with increase in the concentration of doped titanium and strontium ions, mullite phase in the composites increases. The rutile phase (JCPDS No. 211276) is obtained at 1100 ℃ and 1400 ℃ for titanium doped mullite. The

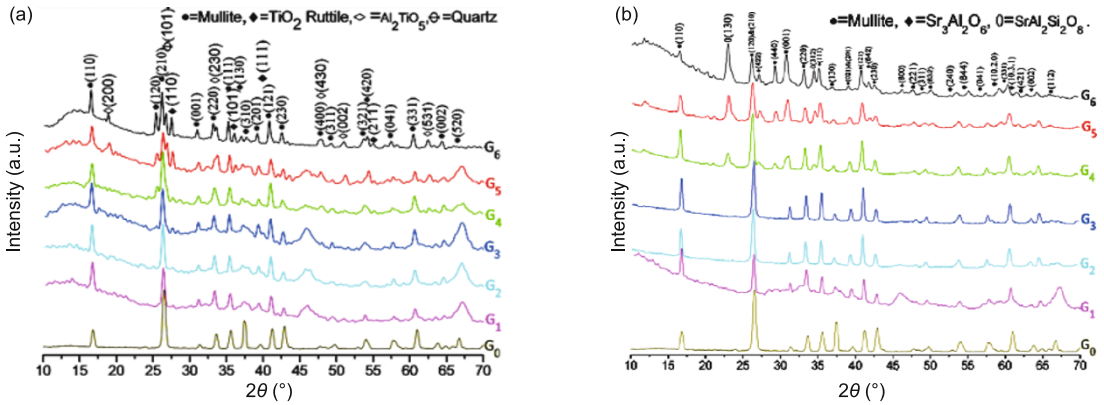

Fig. 1 XRD patterns of (a) titanium and (b) strontium doped mullite precursor gels sintered at 1100 ℃ with increasing doping concentration.

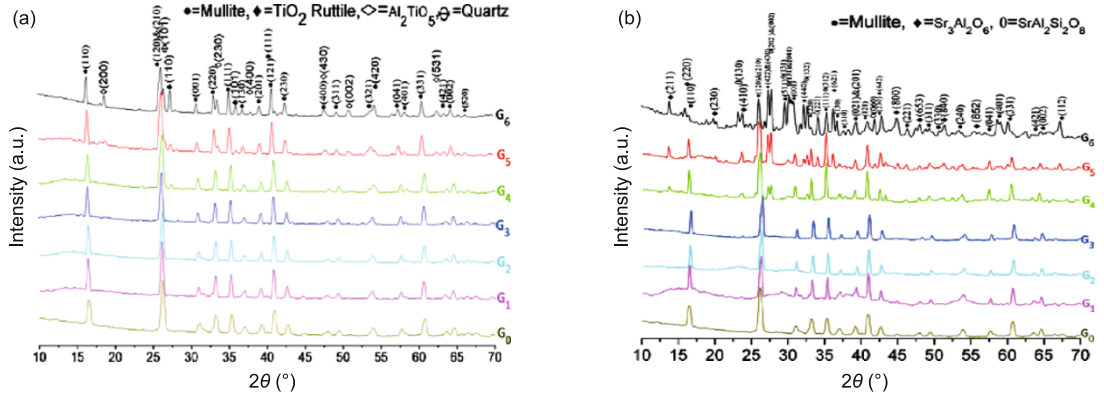

Fig. 2 XRD patterns of (a) titanium and (b) strontium doped mullite precursor gels sintered at 1400 ℃ with increasing doping concentration.

diffractograms show that the amount of mullite formation is more in the case of strontium for all concentrations. The hump at the lower scattering angle shows that glass phase increases with the increase of metal ion concentration. Aluminates and oxide phases are also observed in the diffractograms. The phase variation of the composite is due to the changed concentration of each metal ion and John–Teller distortion [12,13]. Interaction of the metal ions with the alumina and silica components of the gels is responsible for the accelerated transformation to mullite phase. The content of crystalline mullite decreases and the background increases due to the increase of metal ion concentration and the formation of metal silicate and aluminate phases of the samples. The "mineralizing" effect continues for samples G_4 to G_6 with respect to control sample G_0. The "mineralizing" effect of transition metals on phase transformation of mullite is well documented in Refs. [8–14]. Probably there are two possibilities, either complete incorporation of metal ions in mullite structure or dissolution of metal ions in the Si-rich glassy phase. Such amorphous phase increases with the increased metal ions, as an account of decrease of the crystalline phases. The densification of the composite may be due to increased consolidation of the composite because of the molten state of the sintered gel at 1400 ℃ ((Fig. 11(d)) and for the increasing metal ion concentration.

By spectroscopic method, the characteristic stretching and bending modes of vibration of chemical bonds of a sample can be effectively evaluated. 1% of the sample is mixed with spectroscopy grade KBr, pelletized to form disc and analyzed by FTIR spectroscopy. Figure 3 shows the FTIR spectra of titanium and strontium doped sintered gels at 1100 ℃. Mullite gives characteristic bands at wave numbers around 463 cm^{-1}, 542 cm^{-1} (AlO_6), 731 cm^{-1} (AlO_4), 828 cm^{-1} (AlO_4), 1074 cm^{-1} (Si phase), 1130 cm^{-1} (Si–O stretching mode), 1176 cm^{-1} and 1368 cm^{-1} [13,14], and 1226 cm^{-1} and 1450 cm^{-1} for rutile at 1100 ℃ [15]. Strontium doped mullite gives characteristic bands at wave numbers around 465 cm^{-1},

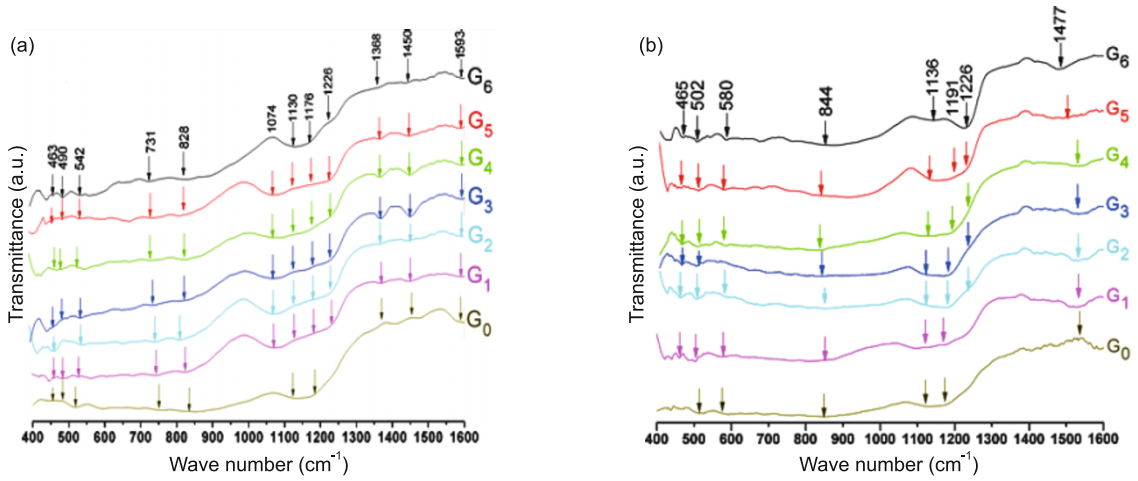

Fig. 3 FTIR patterns in transmittance mode of (a) titanium and (b) strontium doped mullite precursor gels sintered at 1100 ℃ with increasing doping concentration.

502 cm^{-1}, 580 cm^{-1} (AlO_6), 844 cm^{-1} (AlO_4) and 1136 cm^{-1} (Si–O stretching mode), and 1191 cm^{-1} and 1226 cm^{-1} for mullite, and for strontium aluminates ($Sr_3Al_2O_6$) at 1477 cm^{-1} at 1100 ℃ [16].

Figure 4 shows the FTIR spectra of titanium and strontium doped mullite at 1400 ℃. Sanad *et al.* [10,14,17] showed that all the IR spectra obtained for the Y^{3+}, Gd^{3+} doped samples are almost similar to the characteristic peaks of pure o-mullite sample in their overall appearance. For titanium at 1400 ℃, characteristic bands are obtained at wave numbers around 463 cm^{-1}, 509 cm^{-1}, 570 cm^{-1} (AlO_6), 740 cm^{-1} (AlO_4), 820 cm^{-1} (AlO_4), 1114 cm^{-1} (Si–O stretching mode) and 1173 cm^{-1} [16], and 609 cm^{-1}, 1405 cm^{-1} and 1593 cm^{-1} for rutile at 1400 ℃ [15,16]. For strontium at 1400 ℃, characteristic bands are obtained at wave numbers 455 cm^{-1}, 613 cm^{-1} (AlO_6), 700 cm^{-1} (AlO_4), 850 cm^{-1} (AlO_4), 950 cm^{-1} (Si–OH), 1092 cm^{-1} (Si–O phase), 1152 cm^{-1} (Si–O stretching mode) and 1526 cm^{-1} ($Sr_3Al_2O_6$).

The dielectric constant or relative permittivity (ε_r) of each sample is calculated from the capacitance using the formula:

$$\varepsilon_r = (C \times d)/(A\varepsilon_0) \quad (1)$$

where C is the capacitance of the material; d is the thickness of the pellet; A is the area of cross section; and ε_r and ε_0 are the dielectric constant and permittivity of free space, respectively [18,19].

The dielectric properties of materials are used to describe electrical energy storage, dissipation and energy transfer. Electrical storage is the manifestation of dielectric polarization. The variation of dielectric

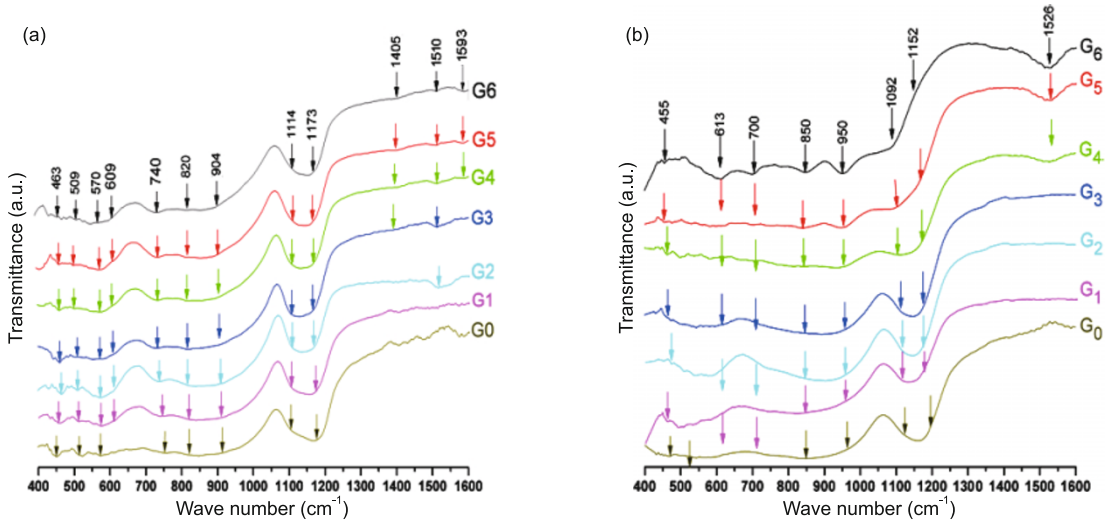

Fig. 4 FTIR patterns in transmittance mode of (a) titanium and (b) strontium doped mullite precursor gels sintered at 1400 ℃ with increasing doping concentration.

constant with frequency of titanium and strontium doped mullite composites at 1100 ℃ are shown in Fig. 5 and similarly at 1400 ℃ in Fig. 6. From the plots, it is clear that in all the cases, dielectric constant decreases with increase in frequency and attains a saturation tendency at 2 MHz for each concentration of doped metal. This behavior of dielectric may be explained qualitatively by the supposition of the mechanism of the polarization process in mullite–titanium/strontium. The electron-hopping model [13] can explain the electrical conduction mechanism. It is known that the effect of polarization is to reduce the field inside the medium. Therefore, the dielectric constant of a substance may be decreased substantially as the frequency is increased [20]. The electronic polarizations can orient themselves with the electric field at the lower frequency range, but at higher frequency the internal individual dipoles contributing to the dielectric constant cannot move instantly. So as frequency of an applied voltage increases, the dipole response is limited and the dielectric constant diminishes [21,22]. The drop in resistivity with frequency predicts the presence of glassy phase /amorphous phase in the mullite structure that may increase the mobility of the ions such as Ti^{4+}/Sr^{2+} and Al^{3+} which find an easy path to move and hence increase the electrical conductivity. Moreover, it is known that the incorporation of transition metals in the periodic lattice of the mullite crystal structure helps in attending a lower band structure [11,14]. The dielectric results of Sanad *et al*.'s data are in good agreements with the data shown at 1100 ℃ and 1400 ℃ of 0.01 M concentration for titanium and strontium ions in the MHz frequency region [10,14,17].

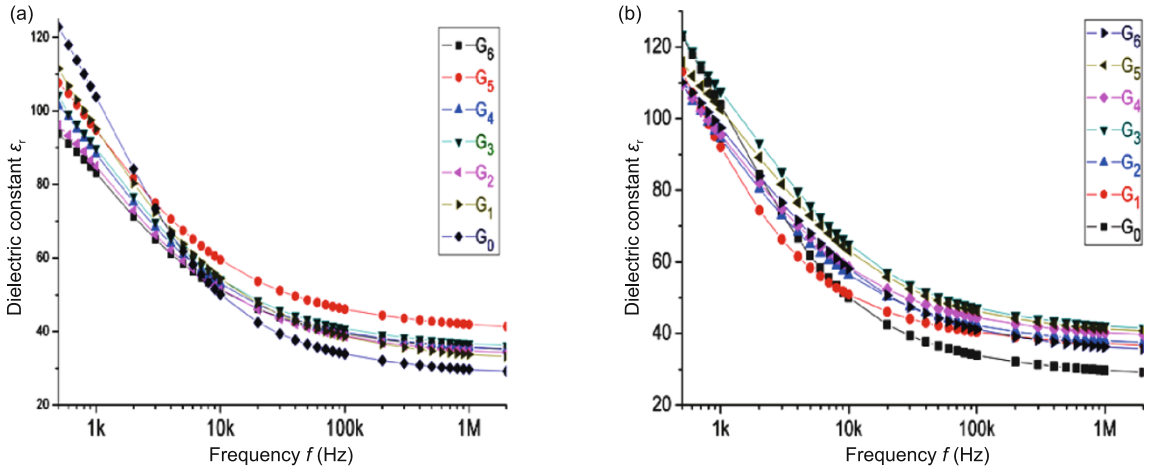

Fig. 5 Frequency response dielectric constant behavior of (a) titanium and (b) strontium doped mullite precursor gels sintered at 1100 ℃ with increasing doping concentration.

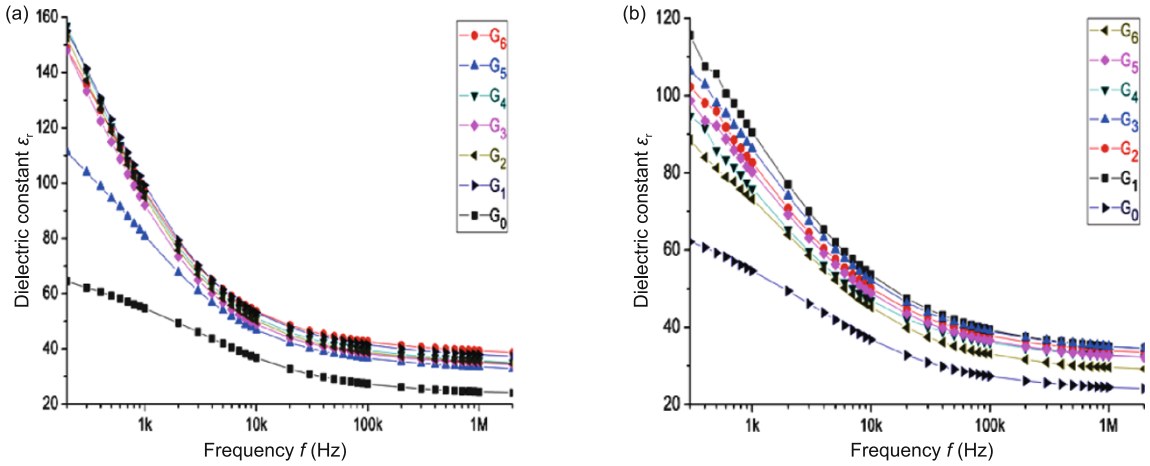

Fig. 6 Frequency response dielectric constant behavior of (a) titanium and (b) strontium doped mullite precursor gels sintered at 1400 ℃ with increasing doping concentration.

The dielectric loss (tanδ) of all samples is measured in the frequency range of 20 Hz to 2 MHz in the room temperature and is graphically shown in Figs. 7 and 8 for 1100 ℃ and 1400 ℃, respectively. It is found that for all samples, tanδ decreases with increasing frequency and reaches constant value at 2 MHz, but initially it increases until 10 kHz. Dissipation factor initially increases maybe due to the greater electronic polarization of the metal ions and also due to the formation of the metal aluminates and oxides. After 10 kHz, the internal electric field will be responsible for the decrement of the dissipation factor. The electronic polarizations can orient themselves with the electric field at the lower frequency range, but at higher frequency, the internal individual dipoles contributing to the dielectric constant cannot move instantly. So as the frequency of an applied voltage increases, the dipole response is limited and the dielectric constant diminishes, and similarly the dielectric loss tanδ decreases.

AC conductivity of the samples is then calculated using the formula:

$$\sigma_{AC} = 2\pi f \tan\delta \varepsilon_r \varepsilon_0 \quad (2)$$

where f is the frequency in Hz; tanδ is the dielectric loss factor; and ε_r and ε_0 are the dielectric constant of the material and permittivity of free space, respectively [23,24].

In σ_{AC} vs. f graphs, a linear increment of AC conductivity with frequency for all doping concentrations is observed for 1100 ℃ (Fig. 9) and 1400 ℃ (Fig. 10). It has been observed that the increment of AC conductivity suddenly jumps from G_4 to G_5. The linearity of the plots follows the frequency

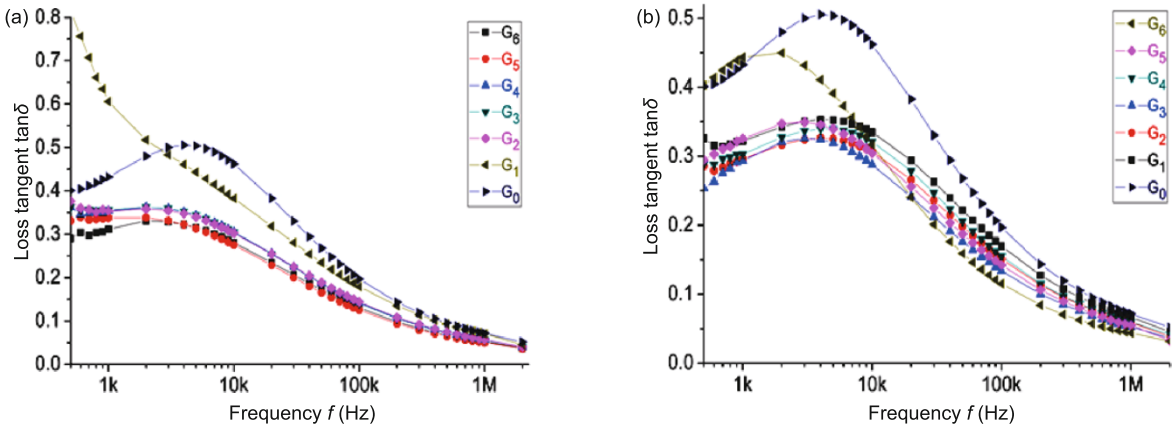

Fig. 7 Frequency response loss tangent behavior of (a) titanium and (b) strontium doped mullite precursor gels sintered at 1100 ℃ with increasing doping concentration.

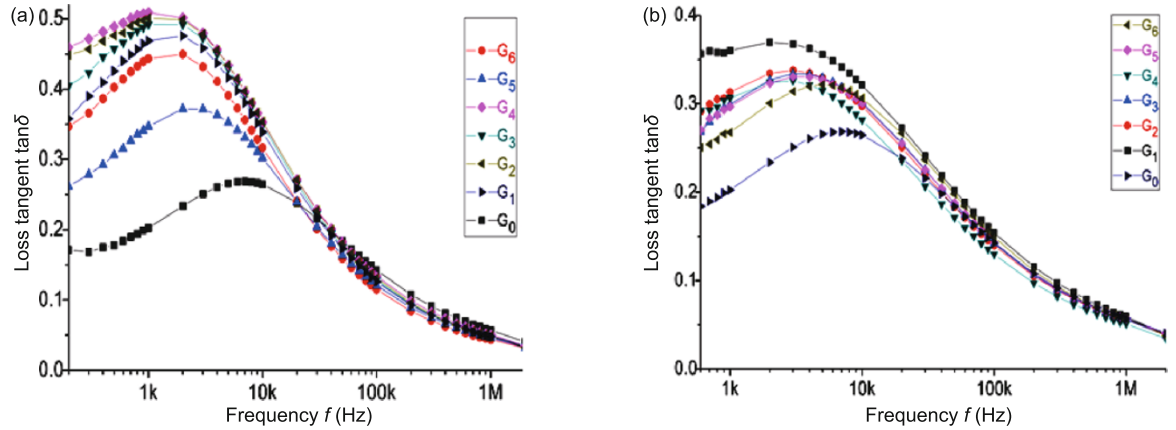

Fig. 8 Frequency response loss tangent behavior of (a) titanium and (b) strontium doped mullite precursor gels sintered at 1400 ℃ with increasing doping concentration.

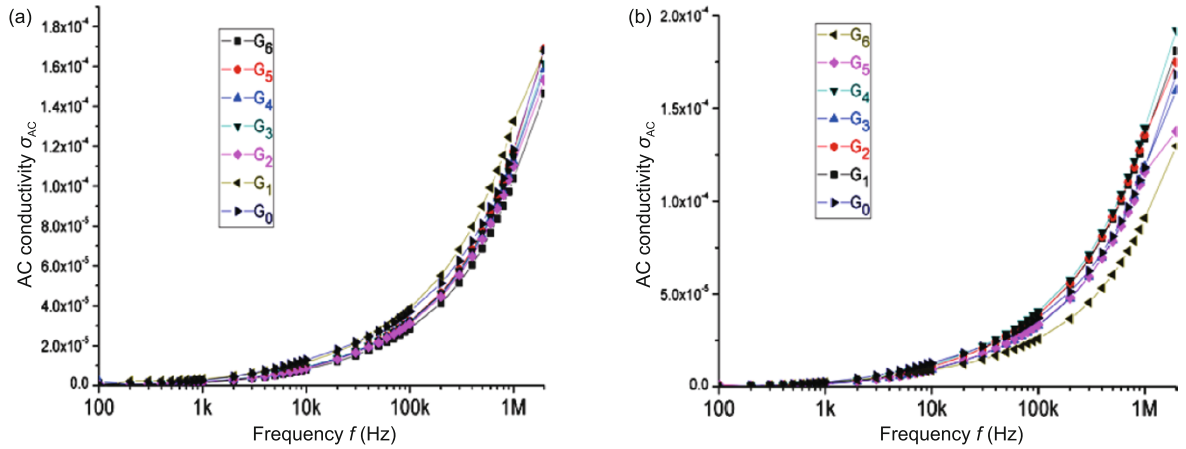

Fig. 9 Frequency response AC conductivity behavior of (a) titanium and (b) strontium doped mullite precursor gels sintered at 1100 ℃ with increasing doping concentration.

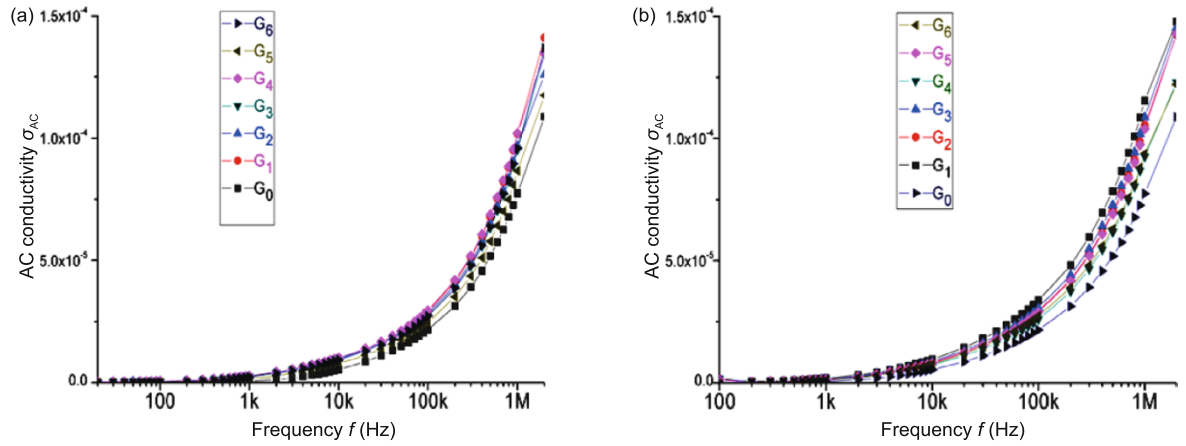

Fig. 10 Frequency response AC conductivity behavior of (a) titanium and (b) strontium doped mullite precursor gels sintered at 1400 ℃ with increasing doping concentration.

dependent part of Jonscher's universal power law which can be represented by the equation:

$$\sigma(\omega) = \sigma_{DC} + \sigma_0 \omega^s \quad (3)$$

where σ_{DC} is the DC (or frequency independent) conductivity; σ_0 is a temperature dependent parameter; and s lies in the range of $0 < s < 1$ [20–25].

The morphology of the mullite particles with G_3 concentration of the doped metal was investigated by FESEM. G_3 sample shows titanium doped mullite nanoparticles of size 50 nm at 1100 ℃ and 100 nm at 1400 ℃ [25]. Similarly for strontium doped mullite, distinct elongated morphology of mullite particles of size 3 μm is embedded in the matrix (Fig. 11). The change in morphology of the sample is due to the combined effect of the doped metals and the sintering temperature. The particles in the case of strontium doped mullite take the shape of whiskers at 1400 ℃ due to the "mineralizing" effect of Sr^{2+} ions.

4 Conclusions

Titanium and strontium doped mullite composites have been synthesized by sol–gel technique, and their phase evolution and dielectric properties have been investigated. The dielectric constant decreased with frequency for all the samples attaining constancy at high frequency, which is a normal behavior for dielectric ceramics. Reported maximum dielectric constants are 24.42 and 37.6 at 1400 ℃ for 0.01 M concentration for titanium and strontium ions at 2 MHz, respectively.

AC conductivity increased with frequency following Jonscher's power law and was found to depend on the amount of glassy phase and concentration of mobile ions present in the composites. The doped mullite may

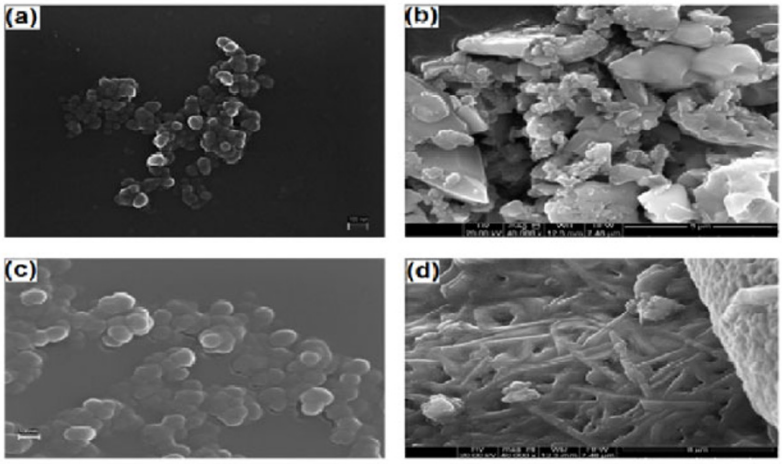

Fig. 11 SEM images of G_3 samples: (a) titanium doped mullite fired at 1100 ℃, (b) strontium doped mullite fired at 1100 ℃, (c) titanium doped mullite fired at 1400 ℃ and (d) strontium doped mullite fired at 1400 ℃.

be used for the fabrication of high charge storing capacitors and also as ceramic capacitors in the pico range.

Acknowledgements

We are grateful to DST and UGC (PURSE program), Government of India, for the financial assistance.

References

[1] Maex K, Baklanov MR, Shamiryan D, *et al*. Low dielectric constant materials for microelectronics. *J Appl Phys* 2003, **93**: 8793.

[2] Ebadzadeh T, Lee WE. Processing–microstructure–property relations in mullite–cordierite composites. *J Eur Ceram Soc* 1998, **18**: 837–848.

[3] Kurihara T, Horiuchi M, Takeuchi Y, *et al*. Mullite ceramic substrate for thin film application. Proceedings of the 40th Electronic Components and Technology Conference, Las Vegas, NV, 1990: 68–75.

[4] Ramakrishnan V, Goo E, Roldan JM, *et al*. Microstructure of mullite ceramics used for substrate and packaging applications. *J Mater Sci* 1992, **27**: 6127–6130.

[5] Viswabaskaran V, Gnanam FD, Balasubramanian M. Mullite from clay–reactive alumina for insulating substrate application. *Appl Clay Sci* 2004, **25**: 29–35.

[6] Camerucci MA, Urretavizcaya G, Castro MS, *et al*. Electrical properties and thermal expansion of cordierite and cordierite–mullite materials. *J Eur Ceram Soc* 2001, **21**: 2917–2923.

[7] Kanka B, Schneider H. Sintering mechanisms and microstructural development of coprecipitated mullite. *J Mater Sci* 1994, **29**: 1239–1249.

[8] Sanad MMS, Rashad MM, Abdel-Aal EA, *et al*. Synthesis and characterization of nanocrystalline mullite powders at low annealing temperature using a new technique. *J Eur Ceram Soc* 2012, **32**: 4249–4255.

[9] Esharghawi A, Penot C, Nardou F. Contribution to porous mullite synthesis from clays by adding Al and Mg powders. *J Eur Ceram Soc* 2009, **29**: 31–38.

[10] Sanad MMS, Rashad MM, Abdel-Aal EA, *et al*. Effect of Y^{3+}, Gd^{3+} and La^{3+} dopant ions on structural, optical and electrical properties of o-mullite nanoparticles. *J Rare Earth* 2014, **32**: 37–42.

[11] Sanad MMS, Rashad MM, Abdel-Aal EA, *et al*. Mechanical, morphological and dielectric properties of sintered mullite ceramics at two different heating rates prepared from alkaline monophasic salts. *Ceram Int* 2013, **39**: 1547–1554.

[12] Roy DS, Bagchi BJ, Bhattacharya AN, *et al*. A comparative study of densification of sol–gel-derived nano-mullite due to the influence of iron, nickel and copper ions. *Int J Appl Ceram Tec* 2013, DOI: 10.1111/ijac.12114.

[13] Roy DS, Bagchi BJ, Das SK, *et al*. Electrical and dielectric properties of sol–gel derived mullite doped with transition metals. *Mater Chem Phys* 2013, **138**: 375–383.

[14] Sanad MMS, Rashad MM, Abdel-Aal EA, *et al*. Optical and electrical properties of Y^{3+} ion

substituted orthorhombic mullite $Y_{(x)}Al_{(6-x)}Si_2O_{13}$ nanoparticles. *J Mater Sci*: *Mater Electron* 2014, **25**: 2487–2493.

[15] Archana J, Navaneethan M, Hayakawa Y. Hydrothermal growth of monodispersed rutile TiO_2 nanorods and functional propertie. *Mater Lett* 2013, **98**: 38–41.

[16] Misevicius M, Scit O, Grigoraviciute-Puroniene I, *et al*. Sol–gel synthesis and investigation of un-doped and Ce-doped strontium aluminates. *Ceram Int* 2012, **38**: 5915–5924.

[17] Sanad MMS, Rashad MM, Abdel-Aal EA, *et al*. Effect of Gd^{3+} ion insertion on the crystal structure, photoluminescence, and dielectric properties of o-mullite nanoparticles. *J Electron Mater* 2014, **43**: 3559–3566.

[18] Patil DR, Lokare SA, Devan RS, *et al*. Studies on electrical and dielectric properties of $Ba_{1-x}Sr_xTiO_3$. *Mater Chem Phys* 2007, **104**: 254–257.

[19] See A, Hassan J, Hashim M, *et al*. Dielectric variations of barium titanate additions on mullite–kaolinite sample. *Solid State Sci Tech* 2008, **16**: 197–204.

[20] Ravinder D, Mohan GR, Prankishan, *et al*. High frequency dielectric behavior of aluminum-substituted lithium ferrites. *Mater Lett* 2000, **44**: 256–260.

[21] Chakraborty AK. Role of hydrolysis water–alcohol mixture on mullitization of Al_2O_3–SiO_2 monophasic gels. *J Mater Sci* 1994, **29**: 6131–6138.

[22] Chakraborty AK. Effect of pH on 980 ℃ spinel phase-mullite formation of Al_2O_3–SiO_2 gels. *J Mater Sci* 1994, **29**: 1558–1568.

[23] Zhang Y, Wu Z, Wang S, *et al*. Density of Li_2TiO_3 solid tritium breeding ceramic pebbles. *Adv Mat Res* 2011, **177**: 310–313.

[24] Oréfice RL, Vasconcelos WL. Sol–gel transition and structural evolution on multicomponent gels derived from the alumina–silica system. *J Sol–Gel Sci Technol* 1997, **9**: 239–249.

[25] Roy DS, Bagchi BJ, Das SK, *et al*. Dielectric and magnetic properties of sol–gel derived mullite–iron nanocomposite. *J Electroceram* 2012, **28**: 261–267.